Title
Live Imaging of the Lung

Journal
Annual Review of Physiology, 76(1)

ISSN
0066-4278

Authors
Looney, Mark R
Bhattacharya, Jahar

Publication Date
2014-02-10

DOI
10.1146/annurev-physiol-021113-170331

Peer reviewed

Published in final edited form as:

Annu Rev Physiol. 2014 ; 76: 431–445. doi:10.1146/annurev-physiol-021113-170331.

Live Imaging of the Lung

Mark R. Looney[1] and **Jahar Bhattacharya**[2]

Mark R. Looney: mark.looney@ucsf.edu; Jahar Bhattacharya: jb39@columbia.edu

[1]Departments of Medicine and Laboratory Medicine, University of California, San Francisco, California 94143

[2]Division of Pulmonary Allergy and Critical Care, Department of Medicine, and Department of Physiology & Cellular Biophysics, Columbia University College of Physicians & Surgeons, New York, New York 10032

Abstract

Live lung imaging has spanned the discovery of capillaries in the frog lung by Malpighi to the current use of single and multiphoton imaging of intravital and isolated perfused lung preparations incorporating fluorescent molecular probes and transgenic reporter mice. Along the way, much has been learned about the unique microcirculation of the lung, including immune cell migration and the mechanisms by which cells at the alveolar-capillary interface communicate with each other. In this review, we highlight live lung imaging techniques as applied to the role of mitochondria in lung immunity, mechanisms of signal transduction in lung compartments, studies on the composition of alveolar wall liquid, and neutrophil and platelet trafficking in the lung under homeostatic and inflammatory conditions. New applications of live lung imaging and the limitations of current techniques are discussed.

Keywords

intravital microscopy; lung slices; two photon; mitochondria; gap junction

INTRODUCTION

The application of microscopy to live tissues has transformed biological understanding in historical and modern times. To a major extent, the success of live microscopy links inextricably to advances in microscope design and selection of tissue preparation. The historical landmark set in 1661 by Malpighi's discovery of pulmonary capillaries is thus clearly attributable to the availability of the compound microscope (1). However, the selection of the frog rather than the mammalian lung also played a determining role in ensuring the success of those early studies (1). Recent advances in live lung microscopy are owed not only to powerful innovations in microscope design and to the availability of novel

DISCLOSURE STATEMENT

The authors are not aware of any affiliations, memberships, funding, or financial holdings that might be perceived as affecting the objectivity of this review.

Author Manuscript

Author Manuscript

Author Manuscript

fluorescent probes, but also to the development of new approaches for viewing the mammalian lung.

Live microscopy of the mammalian lung is problematic because of the considerable lung motion induced by vascular pressure fluctuations in the lung microvascular bed, by the physical impact of the beating heart on the lung, and by lung volume changes due to ventilation. These issues were suitably resolved only recently. We review below pioneering studies by Wearn et al. (2), Terry (3), and more recently Wagner (4) that led to the development of thoracic window approaches for sufficiently stabilizing the lung by means of suction to enable live microscopy during lung ventilation.

We focus on the still nascent field of live lung imaging by first describing the uniqueness of the lung circulation and the history of lung imaging techniques and then reviewing discoveries that have been made with these techniques, including the role of mitochondria in lung immunity, signal transmission at the alveolar-capillary interface, studies on alveolar wall liquid (AWL), and leukocyte and platelet trafficking in the lung. We close with a look to the future and to the challenges that lie ahead in the burgeoning field of live lung imaging.

THE UNIQUENESS OF THE LUNG CIRCULATION

The pulmonary circulation differs in many ways from the systemic circulation. For example, the pulmonary circulation is a low-resistance circuit that must accommodate the full cardiac output; it responds to hypoxia by vasocontricting, whereas hypoxia has a vasodilating effect in the systemic circulation; and the lung's microcirculation is significantly affected by ventilation and by the distension of alveolar units, including a large recruitable capillary pool. The lung's capillary bed is also uniquely organized to maximize gas exchange opportunities. Red blood cells must pass through several alveolar units consisting of 40–100 interconnected capillary segments (5, 6), which is an unusual vascular arrangement that is exclusive to the lung. The vast capillary plexus in the lung consists of segments that vary in diameter from 2 to 15 μm, which is an important feature mandating that red blood cells (5–6 μmin diameter) and neutrophils (6–8 μmin diameter) change their shape to successfully navigate these capillary segments and to exit into the pulmonary venous circulation (7). For anucleate red blood cells, changing their shape is not a difficult task, because these flexible and agile cells contort themselves to squeeze through smaller capillary segments. However, for larger cells like neutrophils, size exclusion is a formidable challenge, as discussed below.

Much of our knowledge of the initial phases of leukocyte rolling, sequestration, firm adhesion, and emigration has come from studies in the systemic circulation. These studies have revealed that selectins are critical for leukocyte rolling and sequestration and that the anatomic site of leukocyte sequestration and emigration is the postcapillary venules (8). However, in the pulmonary circulation, the capillaries are the site of leukocyte sequestration, and the mechanisms of sequestration are selectin independent, as discussed below.

Given these distinct attributes of the pulmonary circulation, it is not possible to image more accessible vascular beds such as the mesentery or cremaster circulation or to conclude that what is observed in the systemic circulation must also happen in the lungs. The lung is unique and must be directly imaged. Many analytic tools in the modern laboratory are well suited for the measurement of global responses during homeostasis and injury conditions, but for the determination of cell-cell interactions both spatially and temporally, live imaging provides unrivaled information. The major obstacle, however, is gaining access to the tissue of interest without disturbing the normal physiology.

LIVE LUNG IMAGING TECHNIQUES

Intravital Lung Imaging Techniques

Intravital microscopy is defined simply as the use of illuminated microscopy in live animals. As applied to the lung, early preparations date back to the 1930s. In 1934, Wearn et al. (2) reported a technique in cats in which a natural thoracic window was created by removing thoracic tissues down to the parietal pleural. By using this technique to image subpleural capillaries, it was discovered that in the lung there is a reserve pool of capillaries that do not always receive perfusion. In 1939, Terry (3) reported the first use of an artificial thoracic window capable of imaging under closed-chest conditions. In the late 1960s,Wagner (4) refined this technique and introduced a major innovation by designing an implantable thoracic window to image the pulmonary circulation of dogs. The technical advance was the introduction of bore holes through which suction could be applied to immobilize the lung and provide enough stabilization for real-time microscopy. Imaging was possible in spontaneously breathing animals, and the thoracic window could be left in place for long-term imaging of an individual animal. Wagner and colleagues used this preparation to define pulmonary capillary transit times (9) and the physiology of capillary recruitment in the lung (10).

The Wagner thoracic window coupled with suction immobilization has been progressively miniaturized for use in rabbits, rats, and mice. For example, in mice, a thoracic window with a 4-mm viewing window has been used in anesthetized, ventilated mice and has been coupled with two-photon microscopy (Figure 1) (11). Other researchers have developed novel intravital approaches. Tabuchi et al. (12) developed a technique to image the mouse lung without artificial contact with the lung's surface. This technique involves creating a 7-mm window in the thoracic wall and covering this window with a transparent membrane glued in situ to create a seal. Next, pleural air is removed with a transdiaphragmal catheter, allowing the lung surface to come into close proximity with the 7-mm viewing window. There is still the issue of tissue movement from mechanical ventilation and cardiac contractions, but because the lung tissue reproducibly returns to the same position, image acquisition can be timed to inspiration or expiration, which effectively excludes intervals of lung displacement. Kreisel et al. (13) described the use of two-photon microscopy in mechanically ventilated mice in which a ring of Vetbond is used to attach the lung tissue to a cover glass in a custom-built chamber maintained at 37°C. Others have clamped the ipsilateral bronchus in the lung being imaged to decrease motion artifact (14).

Intravital lung preparations provide distinct advantages for the experimentalist. These advantages include (*a*) maintenance of a physiological blood circulation; (*b*) the continuous delivery of hematopoietic cells to the lung, including new cells recruited from the bone marrow and secondary lymphoid organs; and (*c*) maintenance of lymph connections in the lung. These advantages come with a price: the challenge of keeping an animal alive under continuous anesthesia and positive-pressure ventilation. But for the right application, intravital lung imaging can be a powerful technique that provides a window into the unique lung microcirculation.

The Isolated Perfused Lung Preparation

The isolated perfused lung (IPL) preparation entails pump perfusion of blood or blood substitutes in ex vivo lungs held at constant inflation at physiological airway and vascular pressures. Widely used as a tool for lung research, the IPL provides a near-motion-free platform for visualization of the alveolar microenvironment by means of wide-angle, confocal, and two-photon microscopy. The stability of the lung surface of the IPL enables application of micropuncture technology, which has been extensively used to determine pressure profiles in microvessels, in the interstitium, and in the alveolar lumen as well as permeability of single microvessels (15). The more recent application of micropuncture is to deliver dyes, antibodies, and other reagents directly to the epithelial or endothelial surfaces of the lung. These real-time fluorescence imaging (RFI) approaches have been particularly useful in the investigation of immune responses in the lung's alveolar-capillary region, the major site of inflammatory lung disease. A recent review addresses RFI with regard to alveolar surfactant secretion and mitochondrial transfer from exogenously instilled mesenchymal stem cells (15). Here we focus on RFI applications that address the spatiotemporal, multicellular profiles of the lung's immune response.

MITOCHONDRIA IN LUNG IMMUNITY

RFI of the IPL preparation has revealed the presence of a set of endothelial cells located at branch-point bifurcations of postcapillary venules that orchestrate the lung's innate immune response (16). These branch-point endothelial cells (BECs) stain negatively for the pericyte marker, α-smooth muscle actin, but positively for the endothelial marker, diacetyl low-density lipoprotein, identifying them as true endothelial cells lying in direct contact with the bloodstream. The relevance to lung immunity is that RFI spontaneously generates Ca^{2+} waves that spread by intercellular communication to the endothelium of upstream capillaries (16), suggesting that BECs oversee Ca^{2+}-dependent metabolic functions of the lung capillary bed, such as nitric oxide (NO) production.

Because BECs express mitochondria at higher density than do endothelial cells of septal capillaries (Figure 2*a*) (17), the mechanical stress of pressure-induced capillary distension (17), or the proinflammatory stress of inflammatory receptor activation (18), increases cytoplasmic Ca^{2+} (cytCa^{2+}) oscillations that in turn increase mitochondrial Ca^{2+} (mitCa^{2+}) (Figure 2*b*). The consequence is increased production of mitochondrial H_2O_2 that diffuses into the cytosol to activate endothelial expression of leukocyte adhesion receptors such as P-selectin. Because these events occur to a greater extent in BECs than at other locations of the pulmonary capillary bed, the lung's immune response initiates with leukocyte accumulation at postcapillary branch points (19). Recent RFI studies on lung capillaries indicate that the endotoxin-induced expression of the leukocyte adhesion receptor ICAM-1 also occurs as a consequence of IP_3-induced endothelial Ca^{2+} oscillations (20, 21).

To quantify a mitochondria-dependent functional outcome in lung microvessels, Rowlands et al. (22) addressed mechanisms of endothelial receptor shedding. Similar to the pressure-induced endothelial cytCa^{2+} oscillations discussed above, TNF-α microinjection in lung capillaries also induced endothelial cytCa^{2+} oscillations, except here TNF-α coupled the cytCa^{2+} oscillations with mitCa^{2+} oscillations to induce release of mitochondrial H_2O_2. The H_2O_2 diffused in the cytosol to activate mechanisms leading to the loss of TNF-α receptor 1 (TNFR1) ectodomains. These mechanisms involved TACE (TNF-α-converting enzyme) because mice lacking endothelial TACE induced mitochondrial H_2O_2 but failed to shed TNFR1. The shedding was also inhibited in microvessels in which mitochondria were made relatively dysfunctional by knockdown of the Rieske iron-sulfur protein. Endothelia of these mitochondria-inhibited microvessels were more prone to expression of leukocyte adhesion receptors as well as to leukocyte accumulation.

An overall conclusion from these findings is that endothelial mitochondria play a role in the lung's immune response. The stress response couples cytCa^{2+} oscillations with mitochondria-dependent defense mechanisms. The extent to which loss of mitochondrial function might contribute to loss of immune defense, and hence to worsening of lung injury during proinflammatory challenge, requires further study.

SIGNAL TRANSMISSION IN LUNG COMPARTMENTS

The understanding of how alveoli communicate with adjoining capillaries to develop the lung's innate immune response lies at the heart of mechanisms underlying inflammatory lung diseases such as acute lung injury (ALI). Sepsis following pneumonitis is a major cause of ALI. Bacterial infection causes transmission of an inflammatory signal from the distal airway to the vascular compartment, resulting in leukocyte migration into the alveolus in 3–4 h (23). In a similar time frame, alveolar macrophages secrete cytokines such as TNF-α that initiate the inflammatory signal by inducing vascular leukocyte recruitment. Application of RFI has facilitated our understanding of how inflammatory signals transfer between and within the alveolar and vascular compartments to orchestrate the immune response.

Because epithelial and endothelial barriers restrict and possibly inhibit direct diffusion of substances between the airway and vascular compartments, cross-compartmental transmission of immune signals likely involves coordinating mechanisms. Using RFI, Kuebler et al. (24) evaluated the role of Ca^{2+} in cross-compartmental signal coordination. Microinjection of TNF-α into the alveolus generated rapid cytCa^{2+} increases in the alveolar epithelium and in the adjoining capillary endothelium, indicating that the passage of the inflammatory signal from alveolus to capillary causes sequential Ca^{2+} increases in each compartment (24). Interestingly, TNF-α injection in the capillary did not increase epithelial cytCa^{2+}. These findings suggest that inflammatory communication in the lung occurs in a vectorial manner such that the direction of signal transfer is uniquely alveolus to capillary. There is little clear-cut evidence that reverse signaling occurs, namely one in which proinflammatory events in the vascular compartment are messaged to alveoli.

RFI studies have addressed paracrine mechanisms that sustain cross-compartmental signal transfer. In Kuebler et al.'s (24) studies, the TNF-α-induced alveolus-capillary signaling was arachidonate dependent in that inhibition of cytosolic phospholipase A_2 blocked the inflammatory response. These studies suggest that Ca^{2+}-induced, basolateral arachidonate release by the alveolar epithelium causes Ca^{2+}-dependent endothelial P-selectin expression and hence leukocyte accumulation in capillaries (24). However, other paracrine mechanisms may also operate. Thus, lung hyperinflation causes Ca^{2+}-dependent basolateral release of epithelial ATP, which then acts on the adjoining endothelium to induce Ca^{2+}-dependent NO release (25). These findings identify a paracrine mechanism in which alveolar ATP couples lung expansion with the steady-state production of endothelial NO.

The application of photolytic release of caged Ca^{2+} in conjunction with RFI enabled the detection of cell-cell communication in alveoli. Ichimura et al. (26) loaded the Ca^{2+} cage NPEGTA into alveoli to evaluate alveolar responses in terms of Ca^{2+} and surfactant secretion. Photolytic uncaging induced these responses not only in the targeted alveolus, but also in neighboring alveoli. Pretreating the alveoli with connexin 43 (Cx43)-inhibiting peptides blocked these conducted responses. Together these findings affirm a previous conclusion (27) that Ca^{2+} increases in a single cell of the alveolar epithelium pass to adjacent alveolar cells through Cx43-containing gap junction channels (GJCs).

The notion of GJCs as facilitators of immune defense carries over to the lung vascular bed, in which photolytic uncaging revealed conduction of evoked Ca^{2+} signals from septal capillaries to distances of ~150 μm from the uncaging site (28). Importantly, Ca^{2+} increases induced in the alveolar capillary bed activated P-selectin expression in venules, indicating that a pathogenic stimulus at one location of the vascular bed can induce a proinflammatory response at a relatively distant location. Parthasarathi (29) quantified microvascular permeability as the peak-to-postwash fluorescence ratio of intravascular FITC dextran and obtained further evidence that microvessels communicate injury signals. Localized lung injury due to alveolar microinjections of acid increased microvascular permeability not only at the site of microinfusion, but also at microvascular locations distant from the injury site at which there was no direct acid contact (29). Inhibiting Cx43 blocked the permeability increases, indicating that Cx43-containing GJCs are responsible for the spread of proinflammatory signals as well as for enhancing permeability in the lung capillary bed.

These RFI studies in alveoli and capillaries, taken together, yield a scenario in which the alveolar epithelium and the vascular endothelium are set up as cellular syncytia that can readily respond to defensive stimuli by intercommunicating Ca^{2+} increases. Such syncytial responses may amplify immune defense across a wider region, even when pathogenic stimuli are relatively localized.

THE ALVEOLAR WALL LIQUID

The thin liquid layer lining the alveolar wall constitutes an important component of the systemic defense against inhaled pathogens. The AWL establishes a liquid phase adjacent to the alveolar epithelium, enabling surfactant phospholipids and proteins to maintain alveolar patency (30) and to establish immune defense (31). Although the presence of the AWL is documented in images obtained by low-temperature electron microscopy (32), RFI afforded a dynamic understanding of AWL formation and its possible role in lung disease.

RFI studies by Jiang et al. (33) show that, when stimulated by cAMP, the cystic fibrosis transmembrane regulator (CFTR) partially drives vascular-alveolar Cl^- transport in the fluid-filled mouse lung. It is proposed that in Cl^--secreting epithelia, as, for example, in airway glands, the basolateral Na^+-K^+-ATPase establishes a Na^+ gradient that drives Cl^- uptake (34) by the basolateral Na^+-K^+-Cl^- cotransporter, raising the intracellular Cl^- potential and thus the Cl^- electrochemical gradient across the cell membrane. CFTR-regulated Cl^- channels in the apical membrane facilitate apical Cl^- secretion (35). To maintain electroneutrality, covectorial Na^+ transport occurs through transcellular or paracellular pathways. Water follows in response to the osmotic gradient established by Na^+ and Cl^- transport.

To test the hypothesis that alveolar Cl^- transport underlies AWL formation, Lindert et al. (36) visualized the AWL in air-inflated mouse IPLs by means of two-photon microscopy. These authors found that microinjection of the water-soluble, membrane-impermeant fluorescent dye FITC dextran in the AWL resulted in spontaneous loss of FITC fluorescence from the alveolar lining, indicating the presence of alveolar water secretion. CFTR inhibitors or Cl^- removal from the IPL perfusate of wild-type mice blocked the secretion. The secretion was absent in *Cftr*-null mice, providing the first direct evidence that CFTR-dependent Cl^- secretion across the alveolar epithelium causes AWL formation. Extrapolating from their RFI data, Lindert et al. calculated an AWL secretion rate of 150 μL/h for the mouse lung. They propose that the AWL is formed by CFTR-driven Cl^- transport at the alveolar epithelium but is then absorbed in the terminal bronchioles. Recent reports indicate that inhibition of alveolar Na^+-K^+-ATPase in association with excessive Cl^- transport into the alveolus can enhance alveolar water secretion, resulting in a predisposition to pulmonary edema (37). Taken together, these findings lead to a new understanding of the role of alveolar ion transport mechanisms, especially with regard to Cl^- fluxes, in the pathophysiology of pulmonary edema.

THE MARGINATED POOL OF NEUTROPHILS IN THE NORMAL LUNG

In humans, neutrophils are the most abundant leukocyte in the peripheral blood and are critical first responders to inflammatory and infectious stimuli (38). Investigators have long searched for a marginated pool of neutrophils that could be rapidly mobilized in response to danger signals. Although marginated pools of neutrophils exist in other organs, studies using lung intravital microscopy have been critical in illuminating the anatomic location of neutrophils in the lung and the unique structural features of the lung that contribute to the lung marginated pool of neutrophils. From a teleological perspective, with open communication to the environment, the lung requires a vigorous innate immune response to the diverse array of potential toxic and infectious exposures. The alveolar macrophage is uniquely positioned to initiate the recruitment of other immune cells into the lung. Positioned just a few micrometers beyond the alveolar space is the lung microcirculation, with its unique circulatory architecture and function (39). The structural features of the lung capillaries (2–15 μm in diameter) and circulating neutrophils (6–8 μm in diameter) would predict that neutrophils would have considerable difficulty passaging from arterioles to venules (7). Using a thoracic window in dogs and high-magnification videomicroscopy to image native unlabeled leukocytes, Gebb et al. (40) determined that roughly half of leukocytes traversed the lung capillary network unimpeded, whereas the other half stopped in capillary segments or junctions. Leukocytes in arterioles were nearly spherical, whereas leukocytes in the capillary bed deformed into elongated shapes and maintained this morphology after entering venules. Doerschuk et al. (7) also showed the leukocyte shape change during capillary perfusion from morphometric measurements of neutrophil shape using light and electron microscopy.

Lien et al. (41) used intravitalmicroscopy in dogs to show that pulmonary capillaries are indeed the anatomic site of neutrophil margination. Neutrophils were fluorescently labeled in vitro, were infused into the pulmonary arteries, and were tracked by using fluorescence videomicroscopy. The fluorescent neutrophils were exclusively sequestered in the pulmonary capillaries; transit times ranged widely from <2 s to >20 min, with a median time of 26 s and a mean time of 6.1 s. Red-blood-cell capillary transit was much faster, ranging from 1.4 to 4.2 s. Neutrophils migrated in hops through the capillaries rather than with slow, continuous migration. This study could be criticized for the ex vivo labeling of neutrophils that could induce activation, which could bias the results toward longer transit times and retention in the pulmonary capillary bed. Kuebler et al. (42) in vivo labeled leukocytes with rhodamine 6G and imaged the subpleural microcirculation in ventilated rabbits and confirmed that the predominant site of leukocyte sequestration is the capillary bed. However, leukocyte rolling was also observed in arterioles and venules, and therefore the authors concluded that all segments of the lung vasculature contribute to the delayed transit of leukocytes through the lung relative to transit of red blood cells. With the availability of neutrophil-specific reporter mice, fluorescent molecular probes, and video-rate optical sectioning imaging, these studies could be repeated to definitively address neutrophil transit times in the lung. In humans, the presence of a lung marginated pool of neutrophils is a more controversial subject (43).

NEUTROPHIL SEQUESTRATION AND EMIGRATION IN THE LUNG

Spatial constraints rather than selectin-mediated rolling seem to be the main determinant of neutrophil retention in lung capillaries. In fact, neither P-selectin nor E-selectin is constitutively expressed by the pulmonary capillary endothelium (44), and although L-selectin is involved in prolonged neutrophil sequestration, it is not required for neutrophil emigration during bacterial pneumonia (45). Worthen et al. (46) elegantly showed that, in response to *N*-formyl-methionylleucyl-phenylalanine, neutrophils stiffened through changes in actin assembly, leading to retention in artificial capillary segments and in rabbit lungs. Because they are sequestered in the lung capillaries, neutrophils can exit the vascular space at this location, which contrasts with the emigration of neutrophils from postcapillary venules in many systemic vascular beds (8). The emigration of neutrophils from the capillary lumen into the alveolar spaces has not been visualized in real time, but technically it should be amenable to modern lung intravital techniques (Figure 3). By using transmission electron microscopy and serial sections of the lung, holes in the basal laminae of capillary endothelial cells and alveolar epithelial type II cells have been observed (47). During bacterial pneumonia, neutrophils migrate through these holes and may use interstitial fibroblasts as guides into the alveolar spaces (48). The paracellular versus transcellular routes of neutrophil migration can be directly visualized with the intravital lung imaging technique.

Doerschuk (44) determined that neutrophil adhesion and migration in the lung, in contrast to these processes in the systemic circulation, occur in both CD11/CD18-dependent and -independent pathways, depending on the inciting stimulus. CD11/CD18-dependent stimuli include *Escherichia coli*, *Pseudomonas aeruginosa*, *E. coli* endotoxin, and IgG immune complexes. CD11/CD18-independent stimuli include *Streptococcus pneumonia*, *Staphylococcus aureus*, hydrochloric acid, hyperoxia, and C5a (44). In mice deficient in CD18 or other leukocyte and endothelial cell integrins, lung imaging could be used to characterize the mechanisms by which neutrophils migrate into the alveolar spaces under different inflammatory states.

Kreisel et al. (13) used two-photon intravital imaging to study mechanisms of neutrophil extravasation in bacterial pneumonia and ischemia-reperfusion after murine lung transplantation. Using LysM-GFP mice, these investigators observed that a large pool of resident lung neutrophils rapidly increased in number after inflammatory challenge. Neutrophils clustered around monocytes, and the depletion of monocytes reduced this clustering phenomenon and reduced neutrophil extravasation. In the mouse orthotopic transplantation model, Kreisel et al. (49) also observed direct interactions between recipient neutrophils and donor dendritic cells. The spatiotemporal observation of cell-cell encounters is hypothesis generating and should spur mechanistic studies to better understand early events in lung inflammation.

PLATELET BIOLOGY IN THE LUNG MICROCIRCULATION

Platelets are gaining increased attention for their roles in lung inflammation and injury (50). The intravital imaging of platelets in the lung has received far less attention than has intravital imaging of neutrophils. Doerschuk et al. (51) used an in vitro radiolabeling approach to determine the characteristics of platelet transit in the lungs compared with transit of leukocytes. There was a 33% extraction of platelets on first pass through the pulmonary circulation compared with 98% extraction for neutrophils. After 10 min of circulation, only 3% of injected platelets remained in the lung compared with 27% of neutrophils. These studies suggested that platelets have less margination in the lung compared with neutrophils, which might have been predicted on the basis of the small size of platelets relative to that of neutrophils and capillary segments. Eichhorn et al. (52) directly visualized platelets in the lung microcirculation by using thoracic windows implanted over rabbit lungs. Platelets were labeled ex vivo with rhodamine 6G and, in selected experiments, were also activated with thrombin prior to intravenous injection. These experiments confirmed the findings by Doerschuk et al. (51) that platelets pass the lung microcirculation with few sustained interactions with the endothelium. The velocity of labeled platelets was similar to that of red blood cells. However, the velocity of thrombin-activated platelets was decreased, and platelets adhered to arterioles, capillaries, and venules (52).

Tabuchi&Kuebler (53) used intravital microscopy in mice to observe platelet circulation in the lungs. Ex vivo carboxyfluorescein diacetate labeling of platelets revealed that some platelets were sequestered in the lung capillaries, and after 60 min of 100% oxygen, significantly more platelets were retained. This oxygen-induced retention of platelets affirms previous studies on oxygen exposure in rats in which platelet sequestration in the lungs preceded neutrophil sequestration (54). These studies are also a cautionary note on the effects of mechanical ventilation with high fractions of oxygen during intravital microscopy. Whenever possible, the fraction of inspired oxygen should be limited by using room air or blended oxygen mixtures.

Platelets are easily activated during the isolation from blood, which may have influenced previous platelet migration studies using ex vivo labeling. In fact, under homeostatic conditions in vivo, platelets physically associate with monocytes and neutrophils via P-selectin and PSGL-1 engagement to form heterotypic aggregates that are of unknown functional significance (55). During inflammatory states such as sepsis (56) and myocardial ischemia (57, 58), the number of monocyte-platelet and neutrophil-platelet aggregates increases, reflecting platelet activation. The migration of these heterotypic aggregates through the lung circulation should be predictably delayed, given the increased size and activation state of the aggregates, although these measurements have not been attempted through intravital lung preparations. Methods to label platelets in vivo include using transgenic animals (CD41-YFP) and fluorescentmonoclonal antibodies against platelet surface markers (CD49b) (59). These methods should avoid unintended platelet activation and have been used to label platelets in the liver sinusoids with or without inflammation.

Lung intravitalmicroscopy is well positioned to answer many unsolved questions on the role of platelets in lung inflammation and injury. In the setting of inflammation, the temporal sequence of neutrophil versus platelet sequestration could be directly visualized. There is evidence from the systemic circulation of endothelial-platelet interactions that secondarily capture leukocytes and conversely endothelial-leukocyte interactions that capture platelets (60). For example, in a mouse model of transfusion-related ALI, intravital imaging of the cremaster circulation revealed that polarized domains of CD11b/CD18 on neutrophils captured circulating platelets (61). Intravital microscopy can also help define the spatial distribution of platelets in the lung in the setting of inflammation and injury, including whether platelets or neutrophil-platelet or monocyte-platelet aggregates migrate into the alveolar spaces. Finally, platelets can trigger neutrophil extracellular trap (NET) formation (62, 63), and this process could be visualized in the lung to determine whether NETs are capable of capturing bacteria and platelets and impede blood flow.

NEW APPLICATIONS OF LIVE LUNG MICROSCOPY

We expect the imaging of cell-cell and cell-environment interactions to proceed at a rapid pace with the availability of transgenic mice and molecular reagents to specifically label cells and their subtypes. The imaging of progenitor cells that are either native to the lung or migrating into the lung should also be possible with this technique. A novel application is the intravital microscopic assessment of gas exchange using multispectral oximetry to produce two-dimensional oxygen saturation mapping (64). With this technique, Tabuchi et al. (65) recently reported that oxygenation begins in precapillary arterioles that are approximately 30 µm in diameter and that, by the time red blood cells encounter alveolar capillaries, approximately 50% of the total oxygen uptake has already occurred. These findings confirm earlier, similar findings of Conhaim & Staub (66), who used reflection spectrometry to assess blood oxygenation in the lung. This type of spatiotemporal mapping of oxygenation can be applied to lung injurymodels to determine the impact of the injury on regional gas exchange.

A new twist to the understanding of connexins in lung signal transmission comes from recent RFI studies by the Kuebler group (67), which addressed the mechanism of hypoxic pulmonary vasoconstriction. This group found that in hypoxia, K^+ channel closure causes depolarization-induced Ca^{2+} entry in endothelia of alveolar capillaries. By means of Cx40- and Cx43-containing GJCs, the Ca^{2+} signal passes from the alveolar to the upstream arteriolar endothelium. Arteriolar constriction ensues as the Ca^{2+}-activated arteriolar endothelium induces paracrine stimulation of the surrounding smooth muscle. By placing the hypoxia-sensing site at alveolar capillaries, and by invoking a role for GJCs, this model offers an elegant solution to the long-standing puzzles of how the lung senses hypoxia and how the resulting signal induces vasoconstriction.

LIMITATION OF LIVE LUNG MICROSCOPY

The major limitation common to all lung surface imaging is depth or *z*-axis penetration. The excitation signal, whether it is single photon or two photon, is rapidly dispersed by the air-liquid interfaces of the lung, and therefore imaging with two-photon microscopy is confined mainly to the first 30–100 µm below the pleural surface (11, 68). Therefore, this technique accesses only the most superficial layer of the alveolar microcirculation. Although the superficial alveolar microvessels display multiple features of the overall pulmonary circulation, such as vascular recruitment (69), hypoxic vasoconstriction (70), and leukocyte recruitment (11), the extent to which there are disparities remains a concern.

LUNG SLICE IMAGING

What techniques are available for the investigator who wishes to visualize arteries, veins, and larger airways? Live lung slices can be prepared to image these deeper structures. This technique involves intratracheally instilling 37°C low-melting-temperature agarose into euthanized mice followed by rapid cooling, and the lungs are then mounted onto a vibratome and cut into 75- to 300-µm slices (71). The lung slices are maintained in media at room temperature until the time for imaging. Slices are placed immobilized in an imager chamber equipped with a heated stage, a peristaltic pump, an in-line heater, and a vacuum. Oxygenated media are perfused over the slices continuously, and tissue viability is excellent over extended periods of time and can be assessed by evaluating ciliary beating in larger airways (72). In fact, lung slices can be maintained in culture for several days, with smooth muscle contraction remaining intact for at least 5 days and ciliary beating for at least 10 days (71). An advantage of using lung slices is that it is relatively easy to stain the slices with dyes or fluorescently conjugated antibodies that are commonly used for flow cytometry or immunofluorescence microscopy (72). A disadvantage is that the effects of lung inflation cannot be addressed in lung slices.

Applications for the lung slice technique include airway (71) and vascular smooth muscle (73) contractility, mucociliary function (74, 75), and allergic responses (76). Ca^{2+} oscillations can be imaged and quantified in studies of airway smooth muscle (71). Thornton et al. (77) used lung slices to track dendritic cells in the lung during homeostasis and in experimental allergic inflammation models. The lung slice model can even be coupled with lung intravital imaging to verify that observations made in the subpleural lung are also present deeper in the lung tissue.

ACKNOWLEDGMENTS

We appreciate the assistance of M.N. Islam in the preparation of the manuscript and also thank Charlotte Summers for her critical review of the manuscript. The work was supported by NHLBI grants HL107386 (to M.R.L.) and HL36024, HL57556, and HL78645 (to J.B.).

LITERATURE CITED

1. West JB. Marcello Malpighi and the discovery of the pulmonary capillaries and alveoli. Am. J. Physiol. Lung Cell. Mol. Physiol. 2013; 304:L383–L390. [PubMed: 23377345]
2. Wearn JTEA, Bromer AW, Barr JW, German WJ, Zschiesche LJ. The normal behavior of the pulmonary blood vessels with observations on the intermittence of the flow of blood in arterioles and capillaries. Am. J. Physiol. 1934; 109:236–256.
3. Terry RJ. A thoracic window for observation of the lung in a living animal. Science. 1939; 90:43–44. [PubMed: 17798138]
4. Wagner WW Jr. Pulmonary microcirculatory observations in vivo under physiological conditions. J. Appl. Physiol. 1969; 26:375–377. [PubMed: 5773180]
5. Hogg JC. Neutrophil kinetics and lung injury. Physiol. Rev. 1987; 67:1249–1295. [PubMed: 3317458]
6. Staub NC, Schultz EL. Pulmonary capillary length in dogs, cat and rabbit. Respir. Physiol. 1968; 5:371–378. [PubMed: 4879179]
7. Doerschuk CM, Beyers N, Coxson HO, Wiggs B, Hogg JC. Comparison of neutrophil and capillary diameters and their relation to neutrophil sequestration in the lung. J. Appl. Physiol. 1993; 74:3040–3045. [PubMed: 8366005]
8. Zarbock A, Ley K. New insights into leukocyte recruitment by intravital microscopy. Curr. Top. Microbiol. Immunol. 2009; 334:129–152. [PubMed: 19521684]
9. Wagner WW Jr, Latham LP, Gillespie MN, Guenther JP, Capen RL. Direct measurement of pulmonary capillary transit times. Science. 1982; 218:379–381. [PubMed: 7123237]
10. Okada O, Presson RG Jr, Godbey PS, Capen RL, Wagner WW Jr. Temporal capillary perfusion patterns in single alveolar walls of intact dogs. J. Appl. Physiol. 1994; 76:380–386. [PubMed: 8175532]
11. Looney MR, Thornton EE, Sen D, Lamm WJ, Glenny RW, Krummel MF. Stabilized imaging of immune surveillance in the mouse lung. Nat. Methods. 2011; 8:91–96. [PubMed: 21151136]
12. Tabuchi A, Mertens M, Kuppe H, Pries AR, Kuebler WM. Intravital microscopy of the murine pulmonary microcirculation. J. Appl. Physiol. 2008; 104:338–346. [PubMed: 18006870]
13. Kreisel D, Nava RG, Li W, Zinselmeyer BH, Wang B, et al. In vivo two-photon imaging reveals monocyte-dependent neutrophil extravasation during pulmonary inflammation. Proc. Natl. Acad. Sci. USA. 2010; 107:18073–18078. [PubMed: 20923880]
14. Hasegawa A, Hayashi K, Kishimoto H, Yang M, Tofukuji S, et al. Color-coded real-time cellular imaging of lung T-lymphocyte accumulation and focus formation in a mouse asthma model. J. Allergy Clin. Immunol. 2010; 125:461–468. e6. [PubMed: 20031194]

15. Bhattacharya J, Matthay MA. Regulation and repair of the alveolar-capillary barrier in acute lung injury. Annu. Rev. Physiol. 2013; 75:593–615. [PubMed: 23398155]
16. Ying X, Minamiya Y, Fu C, Bhattacharya J. Ca^{2+} waves in lung capillary endothelium. Circ. Res. 1996; 79:898–908. [PubMed: 8831516]
17. Ichimura H, Parthasarathi K, Quadri S, Issekutz AC, Bhattacharya J. Mechano-oxidative coupling by mitochondria induces proinflammatory responses in lung venular capillaries. J. Clin. Investig. 2003; 111:691–699. [PubMed: 12618523]
18. Parthasarathi K, Ichimura H, Quadri S, Issekutz A, Bhattacharya J. Mitochondrial reactive oxygen species regulate spatial profile of proinflammatory responses in lung venular capillaries. J. Immunol. 2002; 169:7078–7086. [PubMed: 12471144]
19. Ichimura H, Parthasarathi K, Issekutz AC, Bhattacharya J. Pressure-induced leukocyte margination in lung postcapillary venules. Am. J. Physiol. Lung Cell. Mol. Physiol. 2005; 289:L407–L412. [PubMed: 15879460]
20. Kandasamy K, Bezavada L, Escue RB, Parthasarathi K. Lipopolysaccharide induces endoplasmic store Ca^{2+}-dependent inflammatory responses in lung microvessels. PLoS ONE. 2013; 8:e63465. [PubMed: 23675486]
21. Kandasamy K, Sahu G, Parthasarathi K. Real-time imaging reveals endothelium-mediated leukocyte retention in LPS-treated lung microvessels. Microvasc. Res. 2012; 83:323–331. [PubMed: 22342350]
22. Rowlands DJ, Islam MN, Das SR, Huertas A, Quadri SK, et al. Activation of TNFR1 ectodomain shedding by mitochondrial Ca^{2+} determines the severity of inflammation in mouse lung microvessels. J. Clin. Investig. 2011; 121:1986–1999. [PubMed: 21519143]
23. Skerrett SJ, Martin TR, Chi EY, Peschon JJ, Mohler KM, Wilson CB. Role of the type 1 TNF receptor in lung inflammation after inhalation of endotoxin or *Pseudomonas aeruginosa*. Am. J. Physiol. Lung Cell. Mol. Physiol. 1999; 276:L715–L727.
24. Kuebler WM, Parthasarathi K, Wang PM, Bhattacharya J. A novel signaling mechanism between gas and blood compartments of the lung. J. Clin. Investig. 2000; 105:905–913. [PubMed: 10749570]
25. Kiefmann R, Islam MN, Lindert J, Parthasarathi K, Bhattacharya J. Paracrine purinergic signaling determines lung endothelial nitric oxide production. Am. J. Physiol. Lung Cell. Mol. Physiol. 2009; 296:L901–L910. [PubMed: 19304909]
26. Ichimura H, Parthasarathi K, Lindert J, Bhattacharya J. Lung surfactant secretion by interalveolar Ca^{2+} signaling. Am. J. Physiol. Lung Cell. Mol. Physiol. 2006; 291:L596–L601. [PubMed: 16698857]
27. Ashino Y, Ying X, Dobbs LG, Bhattacharya J. $[Ca^{2+}]_i$ oscillations regulate type II cell exocytosis in the pulmonary alveolus. Am. J. Physiol. Lung Cell. Mol. Physiol. 2000; 279:L5–L13. [PubMed: 10893197]
28. Parthasarathi K, Ichimura H, Monma E, Lindert J, Quadri S, et al. Connexin 43 mediates spread of Ca^{2+}-dependent proinflammatory responses in lung capillaries. J. Clin. Investig. 2006; 116:2193–2200. [PubMed: 16878174]
29. Parthasarathi K. Endothelial connexin43 mediates acid-induced increases in pulmonary microvascular permeability. Am. J. Physiol. Lung Cell. Mol. Physiol. 2012; 303:L33–L42. [PubMed: 22561459]
30. Clements JA. Lung surfactant: a personal perspective. Annu. Rev. Physiol. 1997; 59:1–21. [PubMed: 9074754]
31. Wright JR. Immunomodulatory functions of surfactant. Physiol. Rev. 1997; 77:931–962. [PubMed: 9354809]
32. Bastacky J, Lee CY, Goerke J, Koushafar H, Yager D, et al. Alveolar lining layer is thin and continuous: low-temperature scanning electron microscopy of rat lung. J. Appl. Physiol. 1995; 79:1615–1628. [PubMed: 8594022]
33. Jiang J, Song Y, Bai C, Koller BH, Matthay MA, Verkman AS. Pleural surface fluorescence measurement of Na^+ and Cl^- transport across the air space-capillary barrier. J. Appl. Physiol. 2003; 94:343–352. [PubMed: 12391048]

34. Ballard ST, Inglis SK. Liquid secretion properties of airway submucosal glands. J. Physiol. 2004; 556:1–10. [PubMed: 14660706]
35. Welsh MJ. Intracellular chloride activities in canine tracheal epithelium. Direct evidence for sodium-coupled intracellular chloride accumulation in a chloride-secreting epithelium. J. Clin. Investig. 1983; 71:1392–1401. [PubMed: 6853719]
36. Lindert J, Perlman CE, Parthasarathi K, Bhattacharya J. Chloride-dependent secretion of alveolar wall liquid determined by optical-sectioning microscopy. Am. J. Respir. Cell Mol. Biol. 2007; 36:688–696. [PubMed: 17290033]
37. Solymosi EA, Kaestle-Gembardt SM, Vadasz I, Wang L, Neye N, et al. Chloride transport–driven alveolar fluid secretion is a major contributor to cardiogenic lung edema. Proc. Natl. Acad. Sci. USA. 2013; 110:E2308–E2316. [PubMed: 23645634]
38. Summers C, Rankin SM, Condliffe AM, Singh N, Peters AM, Chilvers ER. Neutrophil kinetics in health and disease. Trends Immunol. 2010; 31:318–324. [PubMed: 20620114]
39. Burns AR, Smith CW, Walker DC. Unique structural features that influence neutrophil emigration into the lung. Physiol. Rev. 2003; 83:309–336. [PubMed: 12663861]
40. Gebb SA, Graham JA, Hanger CC, Godbey PS, Capen RL, et al. Sites of leukocyte sequestration in the pulmonary microcirculation. J. Appl. Physiol. 1995; 79:493–497. [PubMed: 7592208]
41. Lien DC, Wagner WW Jr, Capen RL, Haslett C, Hanson WL, et al. Physiological neutrophil sequestration in the lung: visual evidence for localization in capillaries. J. Appl. Physiol. 1987; 62:1236–1243. [PubMed: 3106311]
42. Kuebler WM, Kuhnle GE, Groh J, Goetz AE. Leukocyte kinetics in pulmonary microcirculation: intravital fluorescence microscopic study. J. Appl. Physiol. 1994; 76:65–71. [PubMed: 8175549]
43. Peters AM. Just how big is the pulmonary granulocyte pool? Clin. Sci. 1998; 94:7–19. [PubMed: 9505861]
44. Doerschuk CM. Mechanisms of leukocyte sequestration in inflamed lungs. Microcirculation. 2001; 8:71–88. [PubMed: 11379793]
45. Doyle NA, Bhagwan SD, Meek BB, Kutkoski GJ, Steeber DA, et al. Neutrophil margination, sequestration, and emigration in the lungs of L-selectin-deficient mice. J. Clin. Investig. 1997; 99:526–533. [PubMed: 9022088]
46. Worthen GS, Schwab B 3rd, Elson EL, Downey GP. Mechanics of stimulated neutrophils: Cell stiffening induces retention in capillaries. Science. 1989; 245:183–186. [PubMed: 2749255]
47. Walker DC, Behzad AR, Chu F. Neutrophil migration through preexisting holes in the basal laminae of alveolar capillaries and epithelium during streptococcal pneumonia. Microvasc. Res. 1995; 50:397–416. [PubMed: 8583953]
48. Behzad AR, Chu F, Walker DC. Fibroblasts are in a position to provide directional information to migrating neutrophils during pneumonia in rabbit lungs. Microvasc. Res. 1996; 51:303–316. [PubMed: 8992230]
49. Kreisel D, Sugimoto S, Zhu J, Nava R, Li W, et al. Emergency granulopoiesis promotes neutrophil-dendritic cell encounters that prevent mouse lung allograft acceptance. Blood. 2011; 118:6172–6182. [PubMed: 21972291]
50. Weyrich AS, Zimmerman GA. Platelets in lung biology. Annu. Rev. Physiol. 2013; 75:569–591. [PubMed: 23043249]
51. Doerschuk CM, Downey GP, Doherty DE, English D, Gie RP, et al. Leukocyte and platelet margination within microvasculature of rabbit lungs. J. Appl. Physiol. 1990; 68:1956–1961. [PubMed: 2361897]
52. Eichhorn ME, Ney L, Massberg S, Goetz AE. Platelet kinetics in the pulmonary microcirculation in vivo assessed by intravital microscopy. J. Vasc. Res. 2002; 39:330–339. [PubMed: 12187123]
53. Tabuchi A, Kuebler WM. Endothelium-platelet interactions in inflammatory lung disease. Vascul. Pharmacol. 2008; 49:141–150. [PubMed: 18625343]
54. Barry BE, Crapo JD. Patterns of accumulation of platelets and neutrophils in rat lungs during exposure to 100% and 85% oxygen. Am. Rev. Respir. Dis. 1985; 132:548–555. [PubMed: 4037528]

55. Vieira-de-Abreu A, Campbell RA, Weyrich AS, Zimmerman GA. Platelets: versatile effector cells in hemostasis, inflammation, and the immune continuum. Semin. Immunopathol. 2012; 34:5–30. [PubMed: 21818701]

56. Gawaz M, Fateh-Moghadam S, Pilz G, Gurland HJ, Werdan K. Platelet activation and interaction with leucocytes in patients with sepsis or multiple organ failure. Eur. J. Clin. Investig. 1995; 25:843–851. [PubMed: 8582450]

57. Furman MI, Barnard MR, Krueger LA, Fox ML, Shilale EA, et al. Circulating monocyte-platelet aggregates are an early marker of acute myocardial infarction. J. Am. Coll. Cardiol. 2001; 38:1002–1026. [PubMed: 11583872]

58. Sarma J, Laan CA, Alam S, Jha A, Fox KA, Dransfield I. Increased platelet binding to circulating monocytes in acute coronary syndromes. Circulation. 2002; 105:2166–2171. [PubMed: 11994250]

59. Jenne CN, Wong CH, Petri B, Kubes P. The use of spinning-disk confocal microscopy for the intravital analysis of platelet dynamics in response to systemic and local inflammation. PLoSONE. 2011; 6:e25109.

60. Zarbock A, Polanowska-Grabowska RK, Ley K. Platelet-neutrophil-interactions: linking hemostasis and inflammation. Blood Rev. 2007; 21:99–111. [PubMed: 16987572]

61. Hidalgo A, Chang J, Jang JE, Peired AJ, Chiang EY, Frenette PS. Heterotypic interactions enabled by polarized neutrophil microdomains mediate thromboinflammatory injury. Nat. Med. 2009; 15:384–391. [PubMed: 19305412]

62. Caudrillier A, Kessenbrock K, Gilliss BM, Nguyen JX, Marques MB, et al. Platelets induce neutrophil extracellular traps in transfusion-related acute lung injury. J. Clin. Investig. 2012; 122:2661–2671. [PubMed: 22684106]

63. Clark SR, Ma AC, Tavener SA, McDonald B, Goodarzi Z, et al. Platelet TLR4 activates neutrophil extracellular traps to ensnare bacteria in septic blood. Nat. Med. 2007; 13:463–469. [PubMed: 17384648]

64. Styp-Rekowska B, Disassa NM, Reglin B, Ulm L, Kuppe H, et al. An imaging spectroscopy approach for measurement of oxygen saturation and hematocrit during intravital microscopy. Microcirculation. 2007; 14:207–221. [PubMed: 17454673]

65. Tabuchi A, Styp-Rekowska B, Slutsky AS, Wagner PD, Pries AR, Kuebler WM. Pre-capillary oxygenation contributes relevantly to gas exchange in the intact lung. Am. J. Respir. Crit. Care Med. 2013; 188:474–481. [PubMed: 23796161]

66. Conhaim RL, Staub NC. Reflection spectrophotometric measurement of O_2 uptake in pulmonary arterioles of cats. J. Appl. Physiol. 1980; 48:848–856. [PubMed: 7451293]

67. Wang L, Yin J, Nickles HT, Ranke H, Tabuchi A, et al. Hypoxic pulmonary vasoconstriction requires connexin 40–mediated endothelial signal conduction. J. Clin. Investig. 2012; 122:4218–4230. [PubMed: 23093775]

68. Perlman CE, Bhattacharya J. Alveolar expansion imaged by optical sectioning microscopy. J. Appl. Physiol. 2007; 103:1037–1044. [PubMed: 17585045]

69. Short AC, Montoya ML, Gebb SA, Presson RG Jr, Wagner WW Jr, Capen RL. Pulmonary capillary diameters and recruitment characteristics in subpleural and interior networks. J. Appl. Physiol. 1996; 80:1568–1573. [PubMed: 8727541]

70. Groh J, Kuhnle GE, Ney L, Sckell A, Goetz AE. Effects of isoflurane on regional pulmonary blood flow during one-lung ventilation. Br. J. Anaesth. 1995; 74:209–216. [PubMed: 7696073]

71. Bergner A, Sanderson MJ. Acetylcholine-induced calcium signaling and contraction of airway smooth muscle cells in lung slices. J. Gen. Physiol. 2002; 119:187–198. [PubMed: 11815668]

72. Thornton EE, Krummel MF, Looney MR. Live imaging of the lung. Curr. Protoc. Cytom. 2012:12.28.1–12.28.12. [PubMed: 25419262]

73. Held HD, Martin C, Uhlig S. Characterization of airway and vascular responses in murine lungs. Br. J. Pharmacol. 1999; 126:1191–1199. [PubMed: 10205008]

74. Delmotte P, Sanderson MJ. Ciliary beat frequency is maintained at a maximal rate in the small airways of mouse lung slices. Am. J. Respir. Cell Mol. Biol. 2006; 35:110–117. [PubMed: 16484686]

75. Kurosawa H, Wang CG, Dandurand RJ, King M, Eidelman DH. Mucociliary function in the mouse measured in explanted lung tissue. J. Appl. Physiol. 1995; 79:41–46. [PubMed: 7559244]

76. Wohlsen A, Uhlig S, Martin C. Immediate allergic response in small airways. Am. J. Respir. Crit. Care Med. 2001; 163:1462–1469. [PubMed: 11371419]

77. Thornton EE, Looney MR, Bose O, Sen D, Sheppard D, et al. Spatiotemporally separated antigen uptake by alveolar dendritic cells and airway presentation to T cells in the lung. J. Exp. Med. 2012; 209:1183–1199. [PubMed: 22585735]

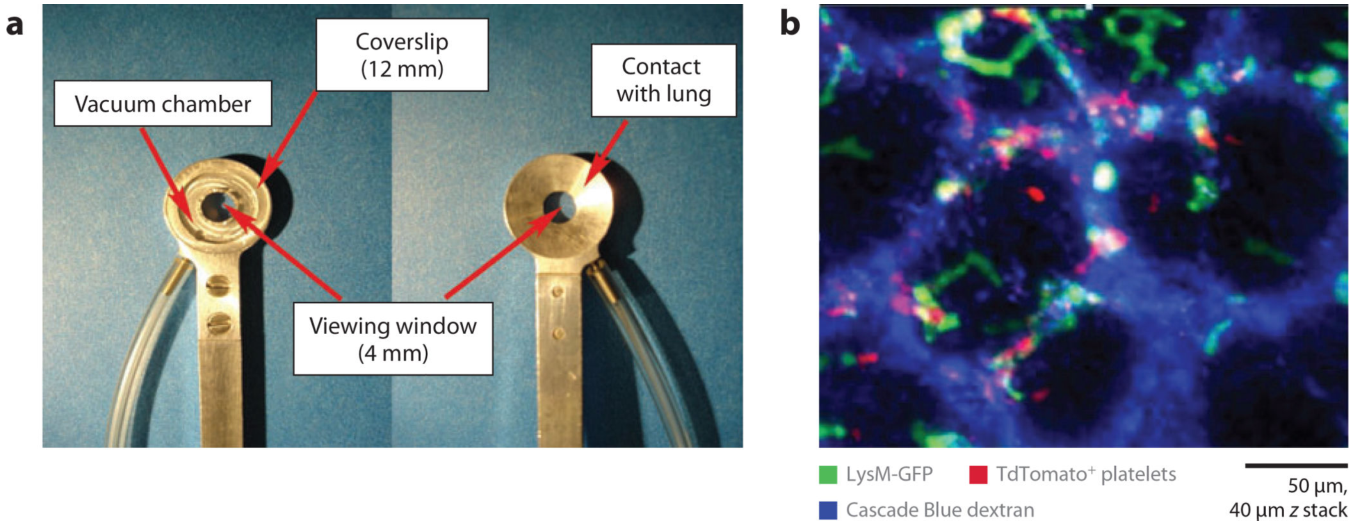

Figure 1.

Stabilized, lung intravital imaging in mice. (*a*) Thoracic window for intravital lung imaging in mice. (*b*) Two-photon microscopy reveals lung alveolar spaces and blood vessels containing neutrophils (*green*) and platelets (*red*). Scale bar, 50 µm, 40 µm *z* stack.

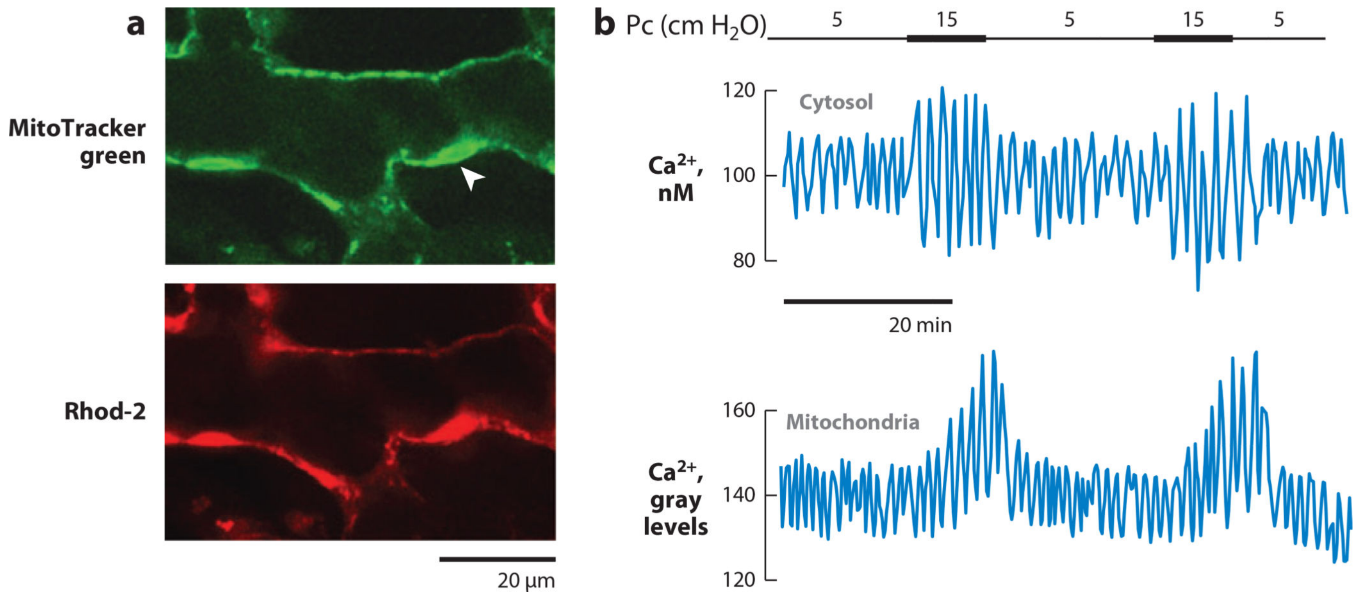

Figure 2.

Real-time fluorescence microscopy of endothelial mitochondria in a lung venular capillary. (*a*) Confocal images show live fluorescence of the mitochondrial density marker MitoTracker green and of the mitochondrial Ca^{2+} dye rhod-2. Mitochondrial density is higher in a branch-point endothelial cell (*arrowhead*) than in other endothelial cells of the capillary. Reprinted with permission from Reference 18. (*b*) Tracings from single capillaries show cytosolic and mitochondrial Ca^{2+} oscillations induced by vascular pressure elevation. Pc denotes capillary pressure. Reprinted with permission from Reference 17.

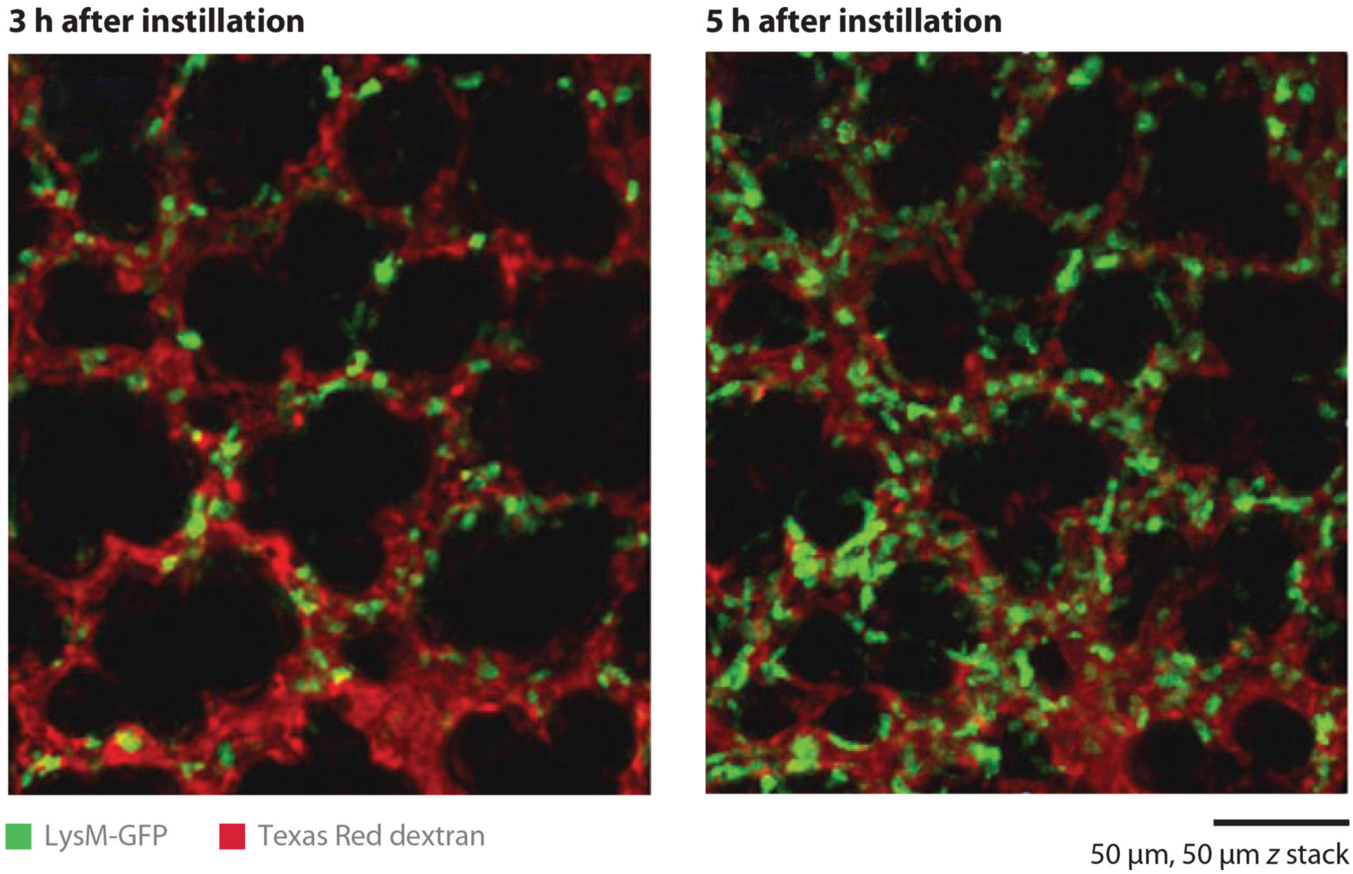

Figure 3.

Lung intravital microscopy in bacterial pneumonia. A LysM-GFP mouse was intratracheally challenged with *Staphylococcus aureus* (2×10^7 cfu) and injected with Texas Red dextran (i.v.). Two screenshots are shown at 3 and 5 h after instillation, revealing progressive neutrophil accumulation in the lung. Scale bar, 50 µm, 50 µm *z* stack.